Proceedings of the
Annual Stability Conference
Structural Stability Research Council
San Antonio, Texas, March 19-22, 2024

Investigations on System Stability of Three-Dimensional Frames

Heera M Titus[1], S Arul Jayachandran[2]

Abstract

With the usage of high-strength steel structures, system instability has become an essential aspect of stability design. In this context, the published research work gravitates toward the nonlinear stability analysis of 3D steel frames. The advanced analysis-based design procedures, as per ANSI/AISC-360, allow the designers to utilize the system's total capacity by directly modeling the effect of imperfections and the spread of inelasticity within the context of a second-order analysis. Hence, a 3D second-order frame analysis must be accurate enough to capture the overall system behavior without excluding any impending failure modes. The present paper develops a novel Total Lagrangian three-dimensional beam element formulation based on the N1-N2 formalism of Mallet & Marcal. Kirchhoff's constraints are enforced in the variational formulation after generating the fundamental kinematic relations of the three-dimensional beam element. The non-vectorial rotations are parameterized using Bryant angles, and the holonomic constraints on beam configuration are enforced. The resulting equations are cast into finite element formulations to develop a novel three-dimensional beam element. Using the developed formulation, a detailed parametric study has been carried out on the stability design provisions of the ANSI/AISC-360 code, and a comparison is made over the conventional stability design using effective length. Two three-dimensional steel frame benchmark problems are chosen to investigate the system stability. The first example is a three-dimensional two-bay-two-story frame in which, depending on the direction of notional loads, the bending moment demand of columns gets resolved into major and minor axes' demands. Usually, notional loads are applied in the direction that provides the greatest destabilizing effect. It is shown that the possible chance of a minor axis demand could become potentially troublesome in the design. Since the problem is a regular frame, the designer may tend to apply notional loads in the direction of applied lateral loads alone, but an additional minor axis demand resulting from the twist might not be captured in the analysis. The second benchmark problem is a one-bay, two-story frame subjected to gravity and lateral loads in two orthogonal directions. It could be shown that instead of doing two separate DAM analyses for each orthogonal direction, a single DAM analysis would suffice in which the notional loads are applied in the direction of the resultant lateral loads at each level. This is in accordance with the guidelines mentioned in ANSI/AISC 360-16. From both the frame problems, it could be concluded that DAM gives accurate results and a realistic picture of force distribution with considerably less effort for the stability design of steel frames.

[1] Graduate Research Assistant, Indian Institute of Technology Madras, heer.titus@gmail.com
[2] Professor, Indian Institute of Technology Madras, arulsteel@gmail.com

1. Introduction

Design methodologies for steel frames must comprehensively account for the nonlinearity in mechanical response inherent in steel structures due to the second-order effects, initial imperfections, and spread of inelasticity. In the Effective Length Method (ELM), this nonlinearity is accounted for by determining effective length factors (K), that are conceptualized based on the elastic stability theory. These factors, coupled with empirical column curves accounting for the effect of geometric imperfections, spread of inelasticity, and residual stresses, are used to assess a beam column axial compressive strength (P_u). Application of ELM becomes tedious for complex geometries because of the need for buckling analysis to identify effective length factors. Thus, the major design philosophies for steel structural systems underwent rapid change by focusing on reducing the design effort. By introducing advanced analysis methods, designers have migrated from a member-based design to a system stability-based design. This also avoids determining effective length factors and using empirical column curves during design. The effect of imperfections, the spread of inelasticity, etc., which used to be accounted for by empirical column curves to determine the member resistance, can be included in the analysis directly.

In the Direct Analysis Method (DAM), the effect of imperfections and stiffness reduction is moved from the resistance side to the analysis side using notional loads and stiffness reduction factors. The design procedure gets exceedingly simplified as it directly identifies the effect of residual stresses, initial imperfections, and spread of inelasticity more consistently in the analysis (Dierlein G 2003; Ingkiriwang and Far 2018; Shankar Nair and Nair 2007; Surovek and Ziemian 2005; Surovek-Maleck et al. 2004a; b) But, the level of accuracy needed for frame analysis may sometimes override the advantages offered by DAM. Before using DAM to design a topology, one should be confident about the advanced analysis tool's capabilities to assess the force distribution under applied loads.

While AISC 360-2016 (ANSI/AISC 360 2016) prescribes that the analysis tool used for DAM must consider all flexural, shear, and axial deformations, it also states that the user can omit certain deformations according to one's engineering judgment regarding the effect these deformations might have on the overall system stability. For example, the shear deformations of a low-rise rise moment frame could be neglected, but the same might not be valid if the elements are stocky and the members are deep with short spans. Most of the modern commercial structural analysis programs can handle second-order effects accurately. But, before relying on an analysis tool, the designer using DAM should be confident about the analysis's capabilities (the included features and, more importantly, the excluded ones). Benchmark problems are necessary as a first-level check to determine whether an analysis tool is sufficient for DAM. The benchmark problems reveal whether different second-order effects are included in the analysis. Structures usually proposed as benchmark problems exhibit significant second-order effects. There are several references in the literature regarding the development of benchmark problems for use in stability design. These include moment frames, braced frames, gable frames, unsymmetric moment frames, unsymmetric braced frames, etc. (Chen and Toma 1994; Surovek and White 2001; Ziemian and Ziemian 2021a; b) Most of the benchmark problems proposed in the literature are in two dimensions. They can be used to assess the in-plane stability of frames. Sometimes, three-dimensional structures are approximated using two-dimensional benchmark problems. When the geometry of the structure itself necessitates a space frame analysis, then 3D benchmark problems are essential (Surovek et al. 2009; Teh 2001, 2004; Ziemian et al. 2018; Ziemian and Abreu 2018).

Even if the frame is planar, certain situations warrant using a 3D analysis tool to predict the failure load of the frame in out-of-plane buckling (Kim et al. 2006; Wongkaew and Chen 2002). The member demands predicted by advanced analysis and the capacities based on a frame with applied notional loads and modified stiffnesses form the interaction equation in ANSI/AISC 360-16 for doubly symmetric beam-column members under uniaxial compression and biaxial bending, given by

$$\frac{P_u}{2\varphi P_n} + \frac{M_{ux}}{\varphi M_{nx}} + \frac{M_{uy}}{\varphi M_{ny}} \leq 1.0, \qquad \frac{P_u}{\varphi P_n} < 0.2 \tag{1a}$$

$$\frac{P_u}{\varphi P_n} + \frac{8}{9}\left(\frac{M_{ux}}{\varphi M_{nx}} + \frac{M_{uy}}{\varphi M_{ny}}\right) \leq 1.0, \qquad \frac{P_u}{\varphi P_n} \geq 0.2 \tag{1b}$$

Hence, it is imperative that numerically accurate three-dimensional beam formulations are essential to have a three-dimensional stability design.

2. A novel three-dimensional Euler Bernoulli Beam Element

In this section, the kinematics of a spatial Euler-Bernoulli beam model is discussed, which is mainly rooted in the following assumptions:

- The cross-section of the beam remains rigid.
- The cross-section of the beam remains perpendicular to the centroidal axis of the beam during deformation.

The implications of the above two assumptions in describing the beam axis and the orientation of the beam cross-section during deformation are explained in subsequent sections.

2.1 Description of beam configurations

The beam configuration described by the centroidal axis is parameterized using the variable '*s*,' which is the arc length of the curve. Let *X*, *Y*, and *Z* be a fixed cartesian frame, where *X(s)* denotes the axis normal to the cross-section.

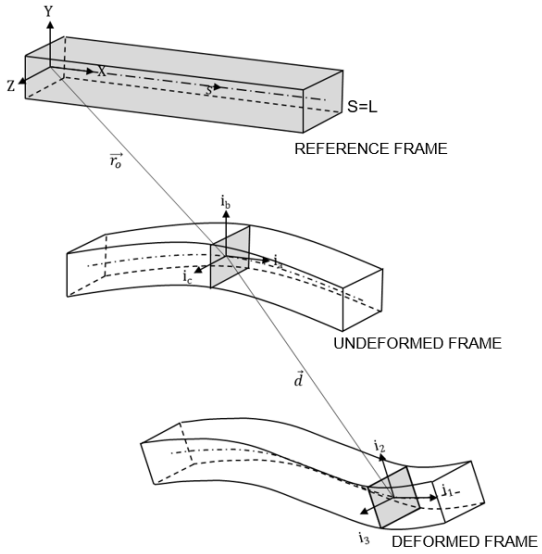

Figure 1: The Total Lagrangian kinematic framework

Any arbitrary point P on the undeformed beam configuration is indicated as:

$$r_0(s,y,z) = r_0(s,0,0) + R_0^T(s)\begin{Bmatrix}0\\y\\z\end{Bmatrix} - I\begin{Bmatrix}0\\Y\\Z\end{Bmatrix} \tag{2}$$

The term $R_0(s)$ defines the orientation of the cross-section in its undeformed configuration. A local frame (i_x, i_y, i_z) is introduced to define the orientation of the cross-section in the undeformed configuration. Similarly, in the deformed reference configuration, the centroidal axis is described as:

$$r(s,y,z) = r(s,0,0) + R(s)\begin{Bmatrix}0\\y\\z\end{Bmatrix} - I\begin{Bmatrix}0\\Y\\Z\end{Bmatrix} \tag{3}$$

where $R(s)$ is defined using the orthonormal local frame given by (i_1, i_2, i_3). The displacement of the centerline is given by:

$$\vec{r} = \vec{r_0} + \vec{d} \tag{4a}$$

$$\vec{d} = \vec{r} - \vec{r}_0 \tag{4b}$$

$R_0(s)$ and $R(s)$ describe the orientation of the local frames with respect to the global cartesian coordinate system.

$$\begin{Bmatrix}i_a\\i_b\\i_c\end{Bmatrix} = [R_0(s)]\begin{Bmatrix}X\\Y\\Z\end{Bmatrix}, \quad \begin{Bmatrix}i_1\\i_2\\i_3\end{Bmatrix} = \left[R_f(s)\right]\begin{Bmatrix}i_a\\i_b\\i_c\end{Bmatrix} \tag{5}$$

$$\begin{Bmatrix}i_1\\i_2\\i_3\end{Bmatrix} = [R(s)]\begin{Bmatrix}X\\Y\\Z\end{Bmatrix}, \text{ where } [R] = \left[R_f\right][R_0] \tag{6}$$

Thus, the deformed configuration is completely characterized by $r(s)$ and $R(s)$.

2.2 Kirchoff's Constraint

For highly slender beams, the shear strains can be assumed to vanish, i.e., during deformation, the plane cross-section remains normal to the centroidal axis. This kinematic constraint of a 3D deformable body helps decide the local frame orientation at each cross-section. If the tangent vector of the deformed centroidal axis $r(s)$ is given by $t(s) = r'(s)$, then the local base vectors i_2 and i_3 will be perpendicular to $t(s)$.

$$\widehat{i_2}.\vec{t}(s) = 0\widehat{i_3}.\vec{t}(s) = 0; \widehat{i_1} = \frac{\vec{t}(s)}{\|\vec{t}(s)\|}; \tag{7}$$

Thus, the beam's cross-section provides a natural way for orienting the local orthonormal frames. Directions of i_2 and i_3 may be chosen as the directions of principal moment of inertia of the cross-section. Kirchoff's constraint can be strongly or weakly enforced in the variational formulation.

2.3 Rotation Parameterization using Bryant Angles

The rotation matrix defines the orientation of a local frame, expressed in terms of suitable sets of coordinates such as Euler angles, Bryant angles, Quaternions, Cartan frames, etc. A spatial rotation can be defined as a series of rotations about the axes of an orthonormal frame. In other words, the rotation matrices can be expressed as the product of three matrices representing three successive

rotations. Several definitions are available to define a spatial rotation depending on the choice of rotation axes for three consecutive rotations.

In this paper, Bryant angles are used to parameterize a spatial rotation. In this case, the $\{i_a\ i_b\ i_c\}^T$ frame is rotated three times to align the axes to $\{i_1\ i_2\ i_3\}^T$. The first rotation α is carried out counter-clockwise about i_a axis. The resulting coordinate system is defined as $i_1''\ i_2''\ i_3'$ systems. Then, the local frame is rotated by β about i_2'' axis to achieve $i_1'\ i_2'\ i_3$ system. Finally, the frame is rotated by ϕ about i_3 to achieve $i_1\ i_2\ i_3$. (Refer Figure 2).

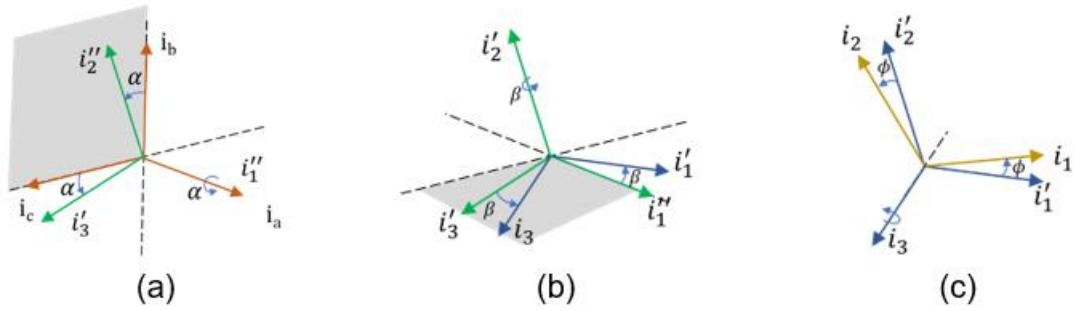

Figure 2: Different stages of rotation (a) Rotation through α about i_a (b) Rotation through β about i_2" (c) Rotation through ϕ about i_3

$$\begin{Bmatrix} i_1'' \\ i_2'' \\ i_3' \end{Bmatrix} = [R_\alpha]\begin{Bmatrix} i_a \\ i_b \\ i_c \end{Bmatrix};\ \begin{Bmatrix} i_1' \\ i_2' \\ i_3 \end{Bmatrix} = [R_\beta]\begin{Bmatrix} i_1'' \\ i_2'' \\ i_3' \end{Bmatrix};\ \begin{Bmatrix} i_1 \\ i_2 \\ i_3 \end{Bmatrix} = [R_\phi]\begin{Bmatrix} i_1' \\ i_2' \\ i_3 \end{Bmatrix} \tag{8a}$$

$$\therefore \begin{Bmatrix} i_1 \\ i_2 \\ i_3 \end{Bmatrix} = [R_\phi][R_\beta][R_\alpha]\begin{Bmatrix} i_a \\ i_b \\ i_c \end{Bmatrix} = [R_f]\begin{Bmatrix} i_a \\ i_b \\ i_c \end{Bmatrix} \tag{8b}$$

$$[R_\alpha] = \begin{bmatrix} 1 & 0 & 0 \\ 0 & \cos\alpha & -\sin\alpha \\ 0 & \sin\alpha & \cos\alpha \end{bmatrix};\ [R_\beta] = \begin{bmatrix} \cos\beta & 0 & \sin\beta \\ 0 & 1 & 0 \\ -\sin\beta & 0 & cos\beta \end{bmatrix};\ [R_\phi] = \begin{bmatrix} \cos\phi & -\sin\phi & 0 \\ \sin\phi & \cot\phi & 0 \\ 0 & 0 & 1 \end{bmatrix} \tag{8c}$$

The rotation matrix associated with Bryant angles is highly nonlinear. $[R_f]$ is singular when $\cos\beta = 0$. The singularity problem is an inherent problem associated with spatial rotations described using three parameters.

2.4 Enforcing the holonomic constraints on beam configuration

The deformation of a nonlinear 3D Euler-Bernoulli beam is described using four independent coordinates (u, v, w, ϕ). In Figure 3, the fixed Cartesian frame xyz is attached to the beam support. i_a, i_b, i_c represent the cross-sectional frame before deformation and $i_1\ i_2\ i_3$ represent the cross-sectional frame after deformation.

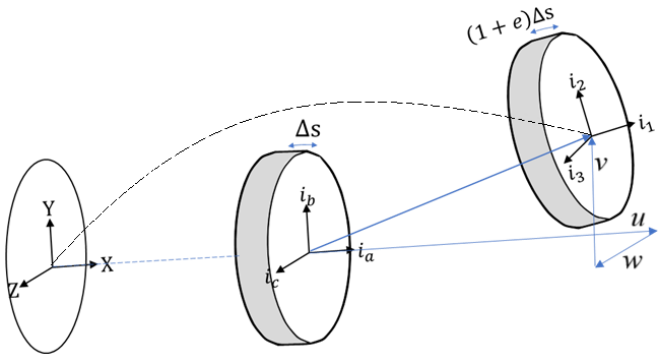

Figure 3: The deformed shape of the configurations during Bryant angle rotations

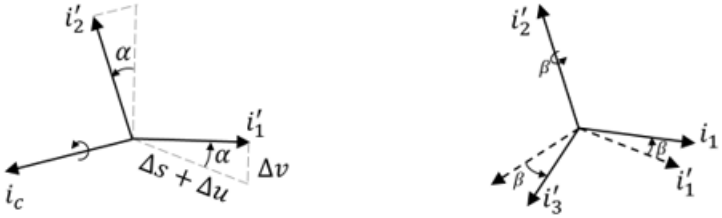

Figure 4: The direction cosines of Bryant angles in terms of displacements

The local frame of the undeformed beam is rotated by α about the axis i_c. The new orientation is denoted by (i'_1, i'_2, i_c).

$$\sin\alpha = \frac{\Delta v}{\sqrt{(\Delta s + \Delta u)^2 + \Delta v^2}} \; ; \; \cos\alpha = \frac{\Delta s + \Delta u}{\sqrt{(\Delta s + \Delta u)^2 + \Delta v^2}} \tag{9}$$

Then, the local frame is rotated by β about i'_2 axis, to form (i_1, i'_2, i'_3).

$$\sin\alpha = \frac{\Delta w}{\sqrt{(\Delta s + \Delta u)^2 + (\Delta v)^2 + (\Delta w)^2}}$$
$$\cos\alpha = \frac{\sqrt{(\Delta s + \Delta u)^2 + (\Delta v)^2}}{\sqrt{(\Delta s + \Delta u)^2 + (\Delta v)^2 + (\Delta w)^2}} \tag{10}$$

For $\lim \Delta s \to 0$,

$$\tan\alpha = \lim_{\Delta s \to 0}\left[\frac{\Delta v}{\Delta s + \Delta u}\right] = \lim_{\Delta s \to 0}\left[\frac{\Delta v/\Delta s}{1 + \frac{\Delta u}{\Delta s}}\right] = \frac{v'}{(1 + u')}$$
$$\tan\beta = \lim_{\Delta s \to 0}\left[\frac{\Delta w}{\sqrt{(\Delta s + \Delta u)^2 + (\Delta v)^2}}\right] = \frac{w'}{\sqrt{(1 + u')^2 + v'^2}} \tag{11}$$

Then, the local frame is rotated by ϕ about i_1 axis to form (i_1, i_2, i_3). ϕ indicates the torsion of the beam axis, whereas α and β are the flexural bending deformations in space. The elastic rotation matrix $[R_f(s)]$ is given by:

$$[R_f] = \begin{bmatrix} 1 & 0 & 0 \\ 0 & \cos\phi & sin\phi \\ 0 & -sin\phi & cos\phi \end{bmatrix} [R_{\alpha\beta}] = \begin{bmatrix} 1 & 0 & 0 \\ 0 & \cos\phi & sin\phi \\ 0 & -sin\phi & cos\phi \end{bmatrix} \begin{bmatrix} \cos\beta & 0 & -\sin\beta \\ 0 & 1 & 0 \\ \sin\beta & 0 & cos\beta \end{bmatrix} \begin{bmatrix} \cos\alpha & \sin\alpha & 0 \\ -\sin\alpha & \cot\alpha & 0 \\ 0 & 0 & 1 \end{bmatrix} \quad (12)$$

$[R_{\alpha\beta}]$ is a function of the displacement gradients. Deformed and undeformed configurations of a nonlinear spatial Euler-Bernoulli beam is described by $[R_f(s)]$. The axial strain of the centroidal axis is given by:

$$e = \sqrt{(1+u')^2 + w'^2 + v'^2} \quad (13)$$

The displacement field is given by:

$$\vec{d}(s,y,z) = \vec{d}(s,0,0) + \left[\left[R_f\right]^T - I\right] \begin{Bmatrix} 0 \\ y \\ z \end{Bmatrix}$$

$$\begin{Bmatrix} u(s,y,z) \\ v(s,y,z) \\ w(s,y,z) \end{Bmatrix} = \begin{Bmatrix} u_0 \\ v_0 \\ w_0 \end{Bmatrix} + \left(\left[R_f\right]^T - [I]\right) \begin{Bmatrix} 0 \\ y \\ z \end{Bmatrix} \quad (14)$$

2.5 Green-Lagrangian Strain Measures

We confine our study to geometrically nonlinear behavior, with the material behaving as linear elastic, thus displaying small strains but finite displacements and rotations. Green-Lagrangian strain tensor is used in this formulation.

$$[\epsilon] = [\epsilon_{ij}] = \begin{bmatrix} \epsilon_{11} & \epsilon_{12} & \epsilon_{13} \\ \epsilon_{21} & \epsilon_{22} & \epsilon_{23} \\ \epsilon_{31} & \epsilon_{32} & \epsilon_{33} \end{bmatrix}$$

$$\epsilon_{ij} = \frac{1}{2}\left[\frac{\partial d_i}{\partial x_j} + \frac{\partial d_j}{\partial x_i} + \frac{\partial d_{im}}{\partial x_i} + \frac{\partial d_m}{\partial x_j}\right] \quad (15)$$

The individual terms can be written by expanding the tensor. The stress-strain relationship governed by Hooke's law is given by:

$$\sigma_{ij} = \begin{Bmatrix} E\epsilon_{ij}\text{ , for } i = j \\ 2G\epsilon_{ij}\text{ , for } i \neq j \end{Bmatrix} \quad (16)$$

The variation of strain energy is given by:

$$\delta U = \int_v [\sigma_{11}\delta\epsilon_{11} + \sigma_{22}\delta\epsilon_{22} + \sigma_{33}\delta\epsilon_{33} + 2\sigma_{12}\delta\epsilon_{12} + 2\sigma_{13}\delta\epsilon_{13} + 2\sigma_{23}\delta\epsilon_{23}]\ dV \quad (17)$$

The strain measure ϵ_{ij} and corresponding stress measure σ_{ij} are functions of u', v', w', and ϕ. The strain energy equation can be reformulated to form the secant stiffness matrices of different order in a staged fashion using the N_1-N_2 formulation of Mallet & Marcal (1968) and Rajasekharan and Murray (1973).

2.6 Mallet and Marcal - N_1-N_2 Formulation

If $\{q\}$ represents the nodal displacement vector of a system with finite degrees of freedom, then the strain-displacement relation is given by:

$$\{\epsilon_i\} = f_i(\{q\}) \tag{18}$$

f_i indicates the dependence of strain measures $\{\epsilon_i\}$ on the nodal displacement $\{q\}$. If the virtual displacements from the equilibrium position are given by $\{\delta q\}$, then the variation in strain components implied by virtual displacements are given by:

$$\delta\epsilon_i = \frac{\partial f_i}{\partial q_k}\delta q_k \tag{19}$$

The principle of virtual work is given by: $\int_v \delta\epsilon_i \sigma_i dV - \delta q_k P_k = 0$ (20)

where, P_k = generalized applied load associated with the direction of q_k. For a linearly elastic material

$$\begin{gathered}\int_v \frac{\partial f_i}{\partial q_k}\delta q_k\, E_{ij}\, f_j\, dV = \delta q_k P_k \\ \delta q_k \left(\int_v \frac{\partial f_i}{\partial q_k}\, E_{ij}\, f_j\, dV\right) = \delta q_k P_k\end{gathered} \tag{21}$$

In the presence of a non-trivial set of virtual displacements,

$$\begin{gathered}\int_v \frac{\partial f_i}{\partial q_k}\, E_{ij}\, f_j\, dV = P_k \\ \frac{\partial}{\partial q_k}\int_v \frac{1}{2}\, E_{ij}\, f_i f_j\, dV = P_k\end{gathered} \tag{22}$$

The strain energy functional of the beam is given by:

$$U = \int_v \frac{1}{2} E_{ij} f_i f_j dV \tag{23}$$

The transcendental terms of strain energy can be expanded in a polynomial form that is amenable to developing secant stiffness matrices. Using Koiter's concept of expressing strain energy as a series:

$$U = U_2 + U_3 + \cdots + U_n + \cdots \tag{24}$$

where, U_2 represents the quadratic terms of strain energy related to the elastic stiffness matrix $[K]$, U_3 represents cubic terms that constitute the first-order displacement matrix $[N_1]$, U_4 represents

the quartic terms related to second order displacement matrix $[N_2]$, and so on. Thus, U_n represents the terms in strain energy expression of degree' n', which will finally constitute $(n\text{-}2)^{th}$ order displacement matrix $[N_{n\text{-}2}]$. The total potential energy is given by:

$$\Pi = \mathrm{U} - \{\mathrm{p}\}^{\mathrm{T}}\{q\} \tag{25}$$

Applying the necessary condition $\frac{\partial \Pi}{\partial P_i} = 0$, and depending on the order of dependence in terms if $U_2, U_3, U_4, \ldots$ on P_i, the equilibrium equation can be written as:

$$[K]\{p\} + \frac{1}{2}[N_1]\{p\} + \frac{1}{3}[N_2]\{p\} + \frac{1}{4}[N_3]\{p\} + \cdots = \{q\} \tag{26}$$

Expanding using the Taylor series, the tangent stiffness relations can be written as,

$$[k]\{\Delta p\} + [N_1]\{\Delta p\} + [N_2]\{\Delta p\} + [N_3]\{\Delta p\} + \cdots = \{\Delta q\} \tag{27}$$

To obtain a general form of secant matrices, irrespective of the discretization of domain and choice of trial functions, the $[N_1] - [N_2]$ method may be applied in a staged manner. If $\{g\}$ represents an array of displacement gradients that appear in strain-displacement relations, then:

$$U = \int_v \{g\}^T \left[\frac{0!}{2!}\left[\hat{k}\right] + \frac{1!}{3!}\left[\widehat{N_1}\right] + \frac{2!}{4!}\left[\widehat{N_2}\right] + \cdots\right]\{g\}\, dV \tag{28}$$

After element discretization, the displacement gradients $\{g\}$ are represented using polynomials in terms of element degrees of freedom $\{\delta\}$

$$\{g\} = \left[\Gamma_{\mathrm{g}\delta}\right]\{\delta\} \tag{29}$$

The element degrees of freedom can be completely transformed into system degrees of freedom.

$$\{\delta\} = \left[\Gamma_{\delta \mathrm{q}}\right]\{q\} \tag{30}$$

2.7 A novel three-dimensional beam element

The proposed beam element for the 3D nonlinear Euler-Bernoulli beam uses the linear and cubic Hermitian interpolation functions for u, v, w, and ϕ .

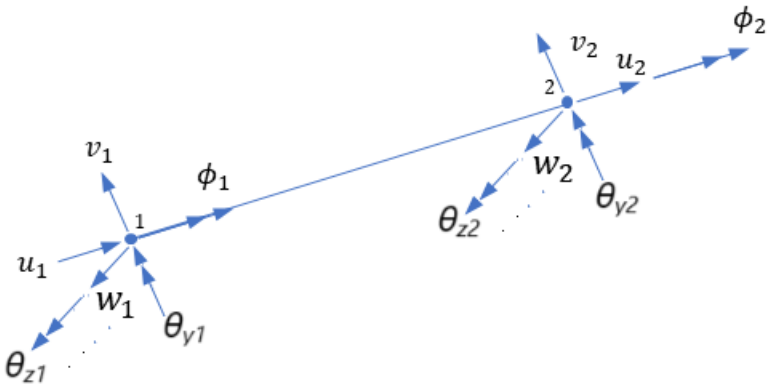

Figure 5: Three-dimensional beam element

$$\{g\}^T = \{u', v', v'', w', w'', \phi, \phi', \phi''\} \tag{31}$$
$$\{q\}^T = \{u_1, v_1, w_1, \phi_1, \theta_{y1}, \theta_{z1}, u_2, v_2, w_2, \phi_2, \theta_{y2}, \theta_{z2}\}^T$$

The linear interpolation functions are given by: -

$$N_1 = 1 - \frac{x}{L},\ N_2 = \frac{x}{L} \tag{32}$$

The cubic Hermitian beam functions are used to discretize flexural degrees of freedom. It should be noted that the secant matrices appear repeatedly in both equilibrium and incremental equations. Both can be formed by simply adjusting the scalar multiples. The secant matrices can be assembled quickly in a computer program 'do' loop.

3. System stability investigations on spatial steel frames

A detailed discussion has been carried out to highlight a particular aspect of the system stability in each example, and comparisons are made between the stability design provisions of the ANSI/AISC-360 code and the conventional stability design of steel frames.

3.1 Notional loads in orthogonal directions of a space frame

In the case of sway frames, depending on the direction of lateral loads, the bending moment demand of columns might get resolved into major axis and minor axis flexure demands. Since notional loads represent the second-order effects of a frame, they shall be applied in the direction that provides the greatest destabilizing effect. The concept of notional loads described in AISC 360 is generally meant for structures that support gravity loads primarily through nominally vertical elements. Regarding the choice of direction of notional loads in the case of a spatial frame, the specification directs the user in Section C2.2b (b) as follows:

"*For most building structures, the requirement regarding notional load direction may be satisfied as follows: for load combinations that do not include lateral loading, consider two alternative orthogonal directions of notional load application, in a positive and a negative sense in each of the two directions, in the same direction at all levels; for load combinations that include lateral loading, apply all notional loads in the direction of the resultant of all lateral loads in the combination.*"

The present problem evaluates the above clause for a sidesway uninhibited moment resisting frame subjected to combined lateral and vertical loading, as shown in Figure 6. In this frame, the beam is also loaded in the middle and is restrained against sidesway at the ends. The frame is loaded such that under the set of applied loads, the frame bends in the x-direction. But, when perturbed at the midpoint of the beam by a very nominal load (0.07 kips), the frame sways considerably in the z-direction. Figure 7 compares the magnitude of deformations at node A in x- and y- y-directions for the given loading. When the beam is lightly loaded, the lateral deformations of the beam are negligible. But, as the beam gets loaded to its total capacity, lateral-torsional deformations of the beam result in significant movement of the frame. While analyzing the frame, even a slight perturbation (≈1/200 of the applied load) in the lateral direction resulted in a significant difference in frame behavior. It must be noted that if the frame was not loaded to its full capacity, this difference might not be noticeable. The lateral loading is applied in the x-direction, and gravity loads act in the -y direction. The columns are oriented in such a way that the columns are bent under lateral load in the x-direction, and buckling of columns may result in deformations in the y-direction. The material is assumed to be linearly elastic, with the modulus of elasticity E = 29,000 ksi, yield stress f_y = 36 ksi, and ν = 0.3.

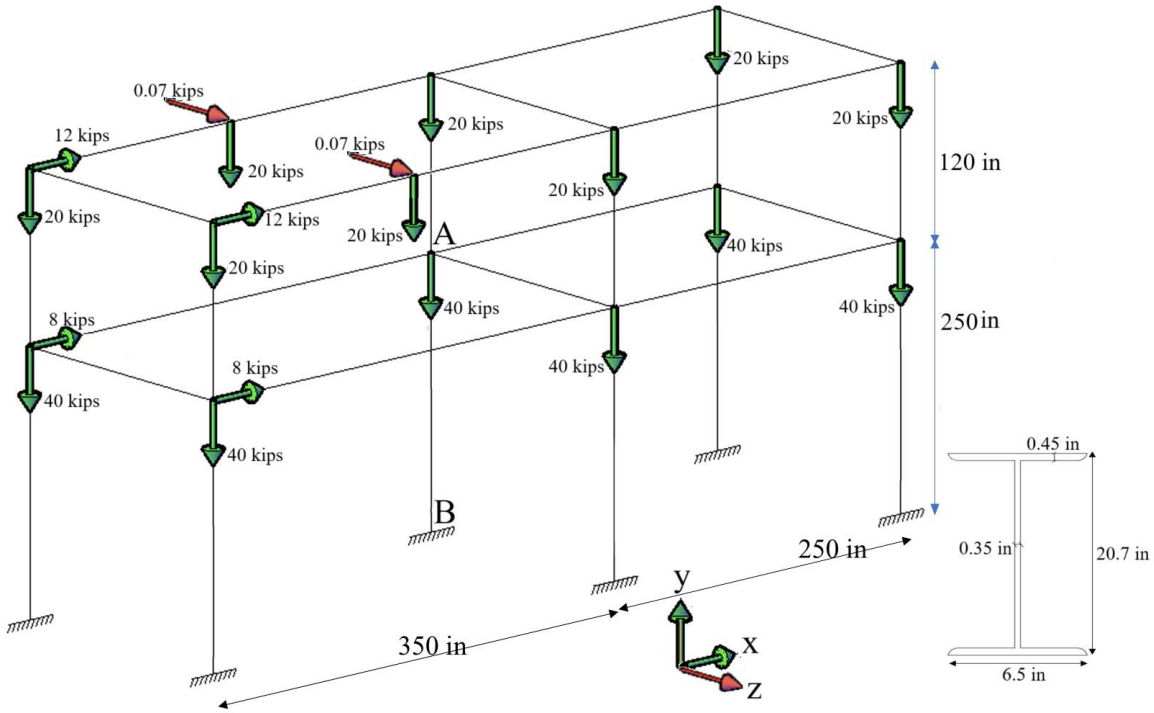

Figure 6: Geometry of a three bay, two story frame

The non-dimensionalized interaction curves and the interaction surface are shown in Figure 8. Column AB is oriented such that major axis flexure under the applied lateral load results in a beam-column subjected to compression and uniaxial flexure. But, if the beam is perturbed to buckle laterally, the entire moment demand gets resolved into major and minor axis flexural demand. Column AB is subjected to uniaxial compression and biaxial flexure when the beam bends laterally. In the case of ELM, the loading is in the x and y directions; hence, no deformations are observed in the z direction.

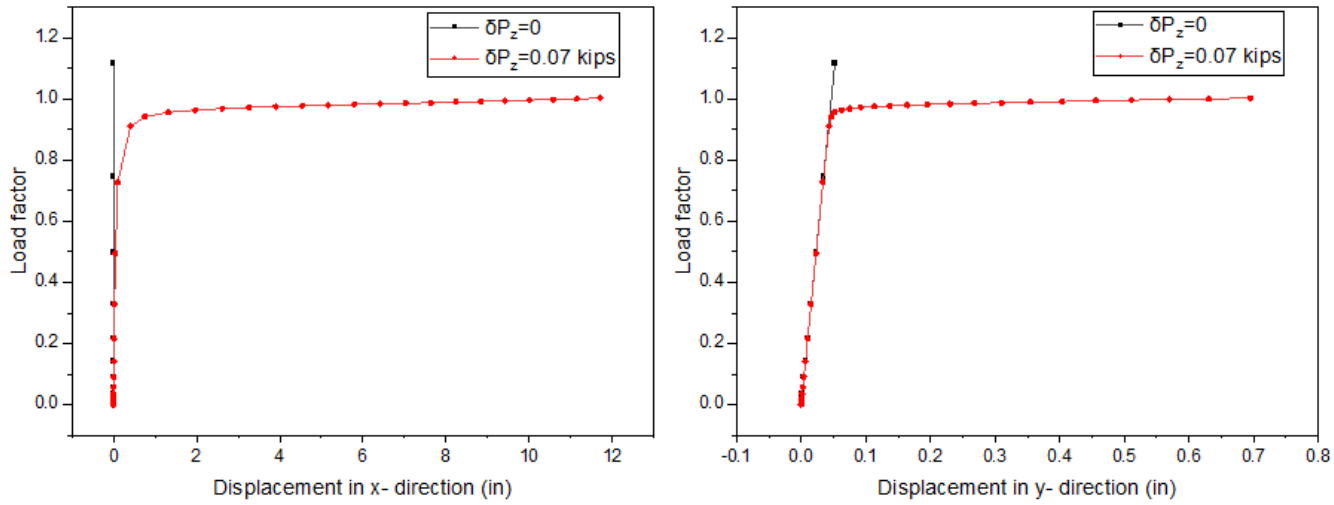

Figure 7: Load v/s displacement graphs at node A in Figure 6

Table 1: Modeling parameters for analysis of cantilever frame in Figure 6

		Parameter	ELM	DAM	
			Model 1	Model 2	Model 3
Modeling for nonlinear analysis		Stiffness reduction factor	1	0.8	0.8
		Notional loads	No	Notional loads in x-direction	Notional loads in z-direction
For column AB in Figure 6	Determination of P_n, M_{nx} and M_{ny}	Effective length factor (K)	0.89	1	1
		Nominal compressive strength, P_n (kips)	92.9	74.5	74.5
		Member major axis flexural strength, M_{nx} (kip.in)	2873.5	2873.5	2873.5
		Minor axis flexural strength, M_{ny} (kip.in)	228.9	228.9	228.9
	Determination of P_u, M_{ux} and M_{uy}	Allowable compressive force, P_u (kips)	64.48	64.41	49.71
		Allowable major axis moment, M_{ux} (kip.in)	960.81	985.18	721.26
		Allowable minor axis moment, M_{uy} (kip.in)	-	-	54.624

The geometrically nonlinear analysis is conducted using the proposed beam element, and its capacity is predicted using Chapter C (DAM) and Appendix 7 (ELM) of ANSI/AISC 360-16. All the supports are assumed to be fixed. W21×44 is used for all the members. Different combinations of notional loads were applied on the frame, three models were studied and the P_u-M_{ux}-M_{uy} curves were plotted against the interaction surface for members under compression and biaxial flexure.

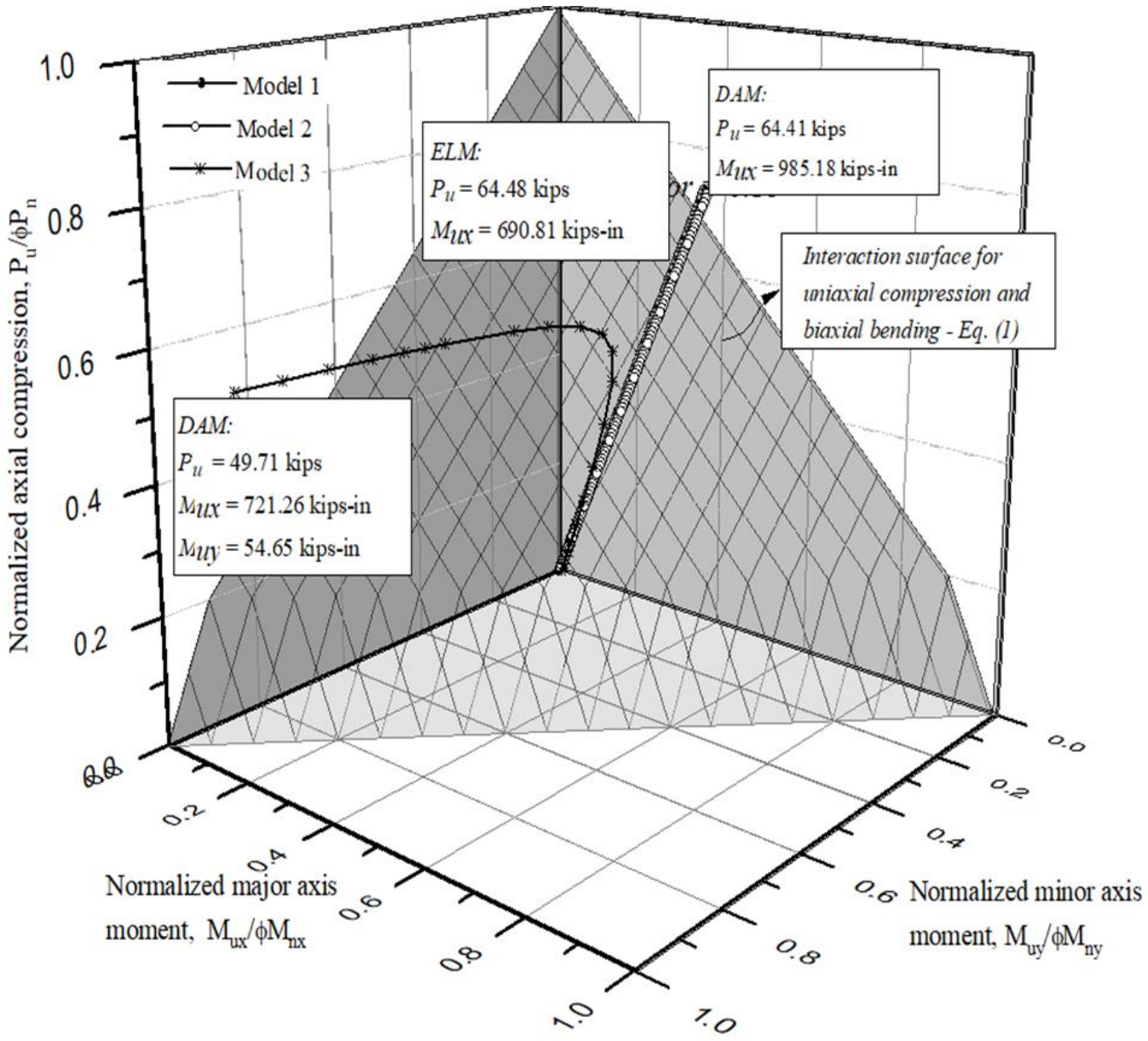

Figure 8: Normalized interaction surface for a member subjected to uniaxial compression and biaxial flexure

The attributes of each of the frame models used for ELM and DAM and the capacities predicted by each model are given in Table 1. While applying DAM, as per Section C2.2b (b) of ANSI/AISC 360-2016, using notional loads in x- the direction alone would suffice. As shown in Table 1, this would result in a capacity very close to ELM. But, if notional loads are applied in z-direction, then the capacity predicted in major axis flexure is much less than that predicted by ELM. When the beam-column reaches its full capacity, even a small twist can cause the total moment demand under applied loads to be resolved into major and minor axes. The column is heavily compressed in ELM and DAM with notional loads in the x-direction, and major axis bending moment-flexural capacity ratio is much less. In DAM with notional loads in the z-direction, the column's capacity

ratios are moderate in compression, major axis, and minor axis flexure. At the same time, the beam has reached its full capacity in lateral-torsional buckling. In situations like this, when the column is not restrained against sway, the major axis demands of the I-shaped member get quickly resolved into significant minor axis demands. When notional loads are applied in orthogonal directions and studied separately, the chance of a potentially troublesome minor axis demand could be identified and could be taken into consideration during design. Since the frame is subjected to lateral loads in the x-direction alone, the user may be inclined to apply notional loads in the x-direction alone, as mentioned in Section C2.2b (b). While this does not significantly impact the design of regular frames, the user should be reminded that the additional minor axis demand resulting from twists could be identified only when notional loads are applied in the z-direction.

3.2 Verification of DAM on a single-bay-two-story frame

Figure 9 shows the geometry of a sway frame primarily subjected to gravity loads. W18×65 sections are used for all members. The material is assumed to be linearly elastic, with E = 200 GPa, and ν=0.3. The geometrically nonlinear analysis is conducted using the proposed beam element, and its capacity is predicted using Chapter C and Appendix 7 of ANSI/AISC 360-16. All

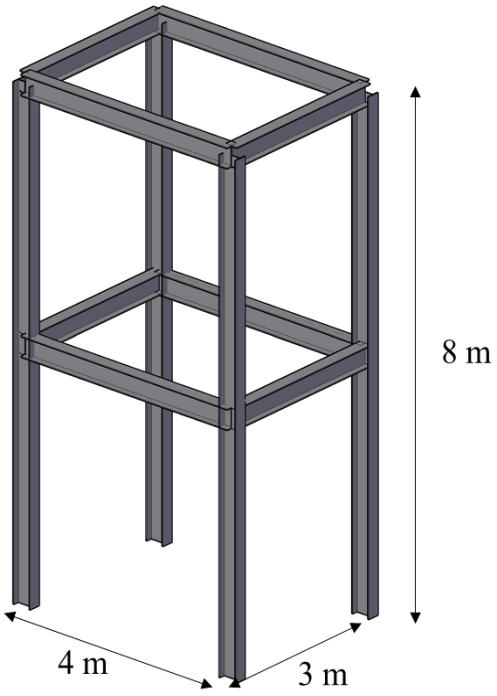

Figure 9: Geometry of a sway frame

the supports are assumed to be fixed. The loading scheme of the frame is as shown in Figure 10. Lateral loads are applied in both directions. The applicability of DAM and ELM on the frame is discussed. For ELM, the effective length factor of the column is 1.8. The capacity ratio of each beam column is calculated under the set of applied loads. The frame primarily fails through flexural buckling of the beam column. Four separate analyses are carried out, and the parameters of each model are tabulated in Table 2.

The notional loads can be applied in each of the orthogonal directions in the case of a spatial frame. But, as stipulated by ANSI/AISC 360-16, for load combinations that include lateral loading, all notional loads are to be applied in the direction of the resultant of all lateral loads in the combination." Four different models are chosen for DAM. The pattern of notional loads applied is shown in Figure 11.

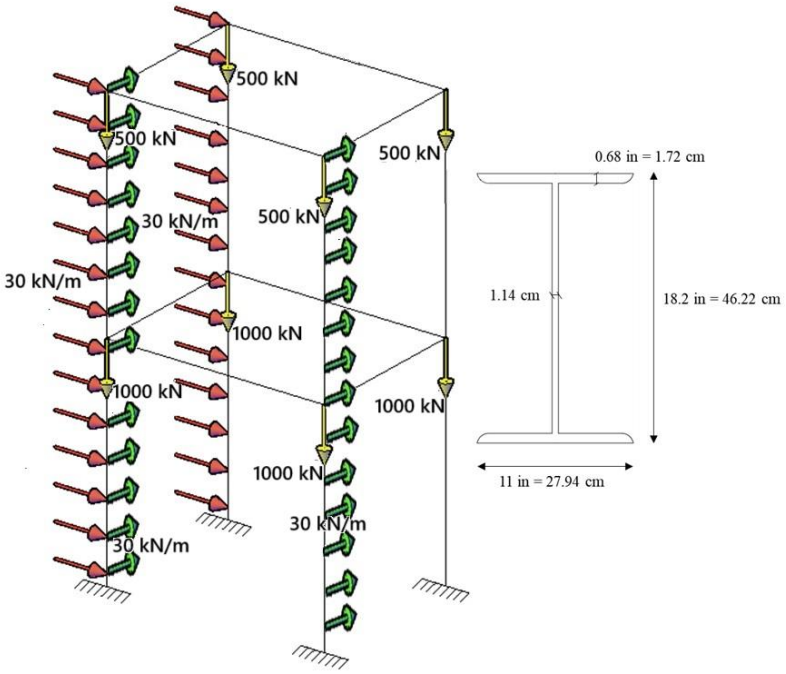

Figure 10: Loading scheme

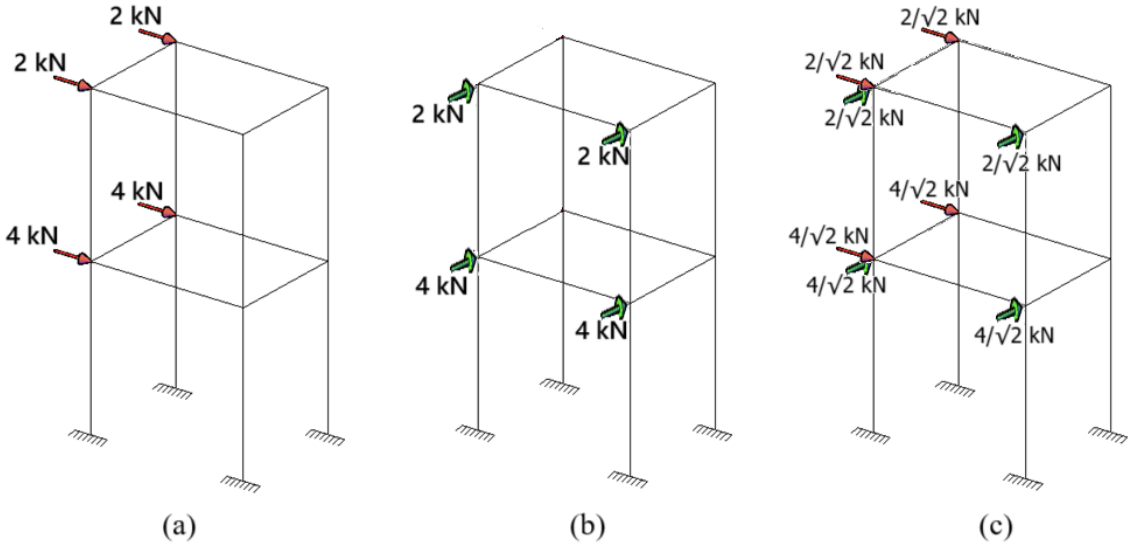

Figure 11: Three different models analyzed for DAM - (a) Model 2, (b) Model 3, and (c) Model 4

Table 2: Modeling parameters for analysis of cantilever frame in Figure 10

	Parameter	ELM	DAM		
		Model 1	Model 2	Model 3	Model 4
Modeling for nonlinear analysis	Stiffness reduction factor	1	0.8	0.8	0.8
	Notional loads	No	Notional loads in x-direction	Notional loads in the z-direction	Notional loads in both x- and z-direction
Determination of P_n and M_n *(kN and kNm)*	Effective length factor (K)	1.8	1	1	1
	Nominal compressive strength,	1364.6	3431.2	3431.2	3431.2
	Member major axis flexural strength, M_{nx}	841.1	841.1	841.1	841.1
	Minor axis flexural strength, M_{ny}	236.4	236.4	236.4	236.4
Determination of P_u and M_{ux} *(kN and kNm)*	Allowable compressive force, P_u	785.8	971.0	972.5	967.2
	Allowable major axis moment, M_{ux}	136.3	168.8	166.5	182.3
	Allowable minor axis moment, M_{uy}	107.9	144.7	142.6	153.4

When notional loads are applied in the ratio of the lateral loads in each direction, the axial compression capacity predicted by DAM is conservative than the other two models. Also, it could be observed that the model with notional loads in both directions predicts the maximum flexure demand out of the four models studied. The effect of lateral load and the resultant sway is accurately accounted for in this model using notional loads. Hence, if a frame is subjected to lateral loads in both the orthogonal directions, instead of applying notional loads in each direction and doing separate analyses for DAM, a single frame with notional loads in the direction of the resultant lateral forces could be applied, resulting in a significant reduction in the design effort. There are significant differences in the column moments between ELM and DAM for frames under heavy gravity loads. It is evident that ELM is more conservative than DAM. But, when flexural demands predicted by a design method is low, connections may also end up underdesigned, which would then require the minimum design criteria proposed in ELM.

4. Summary and Conclusions

The present paper addresses the system stability of 3D steel frames using a nonlinear Euler-Bernoulli beam finite element formulated using the N1-N2 method of Mallet & Marcal formalism. The resulting equations are solved to trace the post-buckling paths. This method is used to investigate the system stability analysis and design of 3D frames undergoing large deformations. Chapter C of ANSI/AISC 360-2016 addresses the primary requirements for the design of structures for stability and permits the use of the direct analysis method (DAM) for all structures. While general analysis requirements stipulated by the code highlight the need for a rigorous advanced analysis tool in determining the required strengths of components, guidelines are given to simplify the analysis and design for structures that support gravity loads primarily through nominally

vertical columns. Two frames are analyzed, emphasizing the use of notional loads. Comparisons are drawn between the ultimate load capacities predicted by DAM and ELM. It could be seen that even when the topology and loading of the frame are symmetric, a 3D frame analysis may be warranted instead of a 2D frame analysis when the primary failure mode is unknown to the designer. The position and direction of notional loads significantly affect the accuracy of DAM. This paper rigorously examines the guidelines for notional loads in ANSI/AISC-360-16 using 3D moment-resisting frames. In DAM, when the notional loads are applied in orthogonal directions in combination with lateral loads, the limit states of lateral-torsional buckling and flexural-torsional buckling should also be considered. These limit states will significantly affect the ultimate behavior of the frame. When a frame is subjected to lateral loads in both the orthogonal directions, instead of applying notional loads in each direction and doing separate analyses for DAM, a single frame with notional loads in the direction of the resultant lateral forces could be applied, resulting in a significant reduction in design effort. The greatest advantage of using DAM is that the second-order moments are amplified to be very close to the actual internal moment distribution of the frame. Thus, the members and connections are designed for higher demands. However, the users of DAM should be aware of the pitfalls associated with modeling geometric imperfections through notional loads and use their engineering judgment during the advanced analysis. The problems presented in this paper are chosen such that the second-order effects of the frame are significant, thereby tending to exaggerate the differences one would typically encounter while adopting the design practices mentioned in ANSI/AISC 360-16.

References

ANSI/AISC 360. 2016. *Specification for Structural Steel Buildings*.

Chen, W. F., and S. Toma. 1994. *Advanced analysis of steel Frames*.

Dierlein G. 2003. *Background and Illustrative Examples on Proposed Direct Analysis Method for Stability Design of Moment Frames*.

Ingkiriwang, Y. G., and H. Far. 2018. “Numerical investigation of the design of single-span steel portal frames using the effective length and direct analysis methods.” *Steel Construction*, 11 (3): 184–191. Ernst und Sohn. https://doi.org/10.1002/stco.201700010.

Kim, S. E., C. M. Uang, S. H. Choi, and K. Y. An. 2006. “Practical advanced analysis of steel frames considering lateral-torsional buckling.” *Thin-Walled Structures*, 44 (7): 709–720. https://doi.org/10.1016/j.tws.2006.08.004.

Shankar Nair, R., and R. S. Nair. 2007. *Stability Analysis and the 2005 AISC Specification NASCC: THE STEEL CONFERENCE. MODERN STEEL CONSTRUCTION*.

Surovek, A. E., B. N. Alemdar, and A. J. Hartwell. 2009. *Three-dimensional Verification and Application of the Direct Analysis Approach*.

Surovek, A. E., and R. D. Ziemian. 2005. “The direct analysis method: Bridging the gap from linear elastic analysis to advanced analysis in steel frame design.” *Proceedings of the Structures Congress and Exposition*, 1197–1210.

Surovek, A., and D. W. White. 2001. *Direct Analysis Approach for the Assessment of Frame Stability: Verification Studies Engineering Creativity View project Direct Analysis and Steel Frame Stability View project*.

Surovek-Maleck, A. E., M. Asce, D. W. White, and A. M. Asce. 2004a. “Alternative Approaches for Elastic Analysis and Design of Steel Frames. I: Overview.” https://doi.org/10.1061/ASCE0733-94452004130:81186.

Surovek-Maleck, A. E., M. Asce, D. W. White, and A. M. Asce. 2004b. “Alternative Approaches for Elastic Analysis and Design of Steel Frames. I: Overview.” https://doi.org/10.1061/ASCE0733-94452004130:81186.

Teh, L. H. 2001. *Cubic beam elements in practical analysis and design of steel frames*. *Eng Struct*.
Teh, L. H. 2004. “Beam element verification for 3D elastic steel frame analysis.” *Comput Struct*, 82 (15–16): 1167–1179. https://doi.org/10.1016/j.compstruc.2004.03.022.
Wongkaew, K., and W.-F. Chen. 2002. *Consideration of out-of-plane buckling in advanced analysis for planar steel frame design*. *J Constr Steel Res*.
Ziemian, C. W., and R. D. Ziemian. 2021a. “Efficient geometric nonlinear elastic analysis for design of steel structures: Benchmark studies.” *J Constr Steel Res*, 186. Elsevier Ltd. https://doi.org/10.1016/j.jcsr.2021.106870.
Ziemian, C. W., and R. D. Ziemian. 2021b. “Steel benchmark frames for structural analysis and validation studies: Finite element models and numerical simulation data.” *Data Brief*, 39. Elsevier Inc. https://doi.org/10.1016/j.dib.2021.107564.
Ziemian, R. D., and J. C. B. Abreu. 2018. “Design by advanced analysis – 3D benchmark problems: Members subjected to major- and minor-axis flexure.” *Steel Construction*, 11 (1): 24–29. Wiley-Blackwell. https://doi.org/10.1002/stco.201810011.
Ziemian, R. D., J. C. Batista Abreu, M. D. Denavit, and T.-J. L. Denavit. 2018. “Three-Dimensional Benchmark Problems for Design by Advanced Analysis: Impact of Twist.” *Journal of Structural Engineering*, 144 (12). American Society of Civil Engineers (ASCE). https://doi.org/10.1061/(asce)st.1943-541x.0002224.